# Supplementary materials

## Supplemental Methods

### Cell culture

Human cells (including SW480, HCT116, SW620, HT29 and 293T) and murine CT26 cells were purchased from Cell Bank, Type Culture Collection, Chinese Academy of Sciences (CBTCCCAS, China). Human SW48 cells and murine MC38 cells were purchased from American Type Culture Collection (ATCC, USA). All human cells and murine MC38 cells were maintained in Dulbecco's Modified Eagle Medium (GIBCO, USA). Murine CT26 cells were cultured in RPMI 1640 medium (HyClone, China). All cell lines were supplemented with 10% fetal bovine serum (BI, Israel) and regularly tested for mycoplasma contamination by CBTCCCAS.

### RNA interference

For transient transduction, cells were transfected with plasmids or small interfering RNA (siRNA) using Lipofectamine 2000 transfection reagent (Invitrogen, USA). The sequences of the plasmids and siRNA used in this study are listed in Table S1. To establish stable cell lines, cells were infected with the indicated lentiviruses and then selected with puromycin, hygromycin B or blasticidin S.

### Immunofluorescence

After washing with cold PBS 3 times, the cells were fixed with 4% paraformaldehyde and permeabilized with 0.3% Triton X-100 (Beyotime, Shanghai,

China) for 15 min. Then, the cells were blocked with 5% BSA and incubated with the indicated antibodies overnight. On the next day, the cells were stained with secondary antibody for 2 h at room temperature. DAPI was used to counterstain the nucleus. Images were visualized by a confocal microscope (Leica, Germany), and data were quantified by ImageJ.

**Proximity ligation assay (PLA)**

PLA was performed using the Duolink® In Situ Red Starter Kit (Sigma, USA). Briefly, cells with the indicated treatments were washed 3 times with cold PBS and then fixed in 4% paraformaldehyde. After blocking with blocking solution for 30 min, the cells were incubated with anti-H-2K$^{b}$, anti-CEMIP or anti-clathrin for 2 h at 37 °C. Cells were then incubated with PLA probe PLUS and PLA probe MINUS for 1 h at 37 °C, followed by incubation with ligation-ligase and amplification-polymerase. After that, the cells were stained with DAPI, and the PLA signals were observed by confocal microscopy (Leica, Germany).

**Western blotting and immunoprecipitation**

For western blotting, cells were lysed with ice-cold RIPA buffer to extract the protein. Then, proteins were separated using a 10% SDS–PAGE gel and transferred to PVDF membranes. After blocking with 5% skim milk, PVDF membranes were immunoblotted with the indicated antibodies (Supplementary Table 2). After incubation with HRP-conjugated secondary antibody, bands were captured using enhanced chemiluminescence. Protein quantification was normalized using GAPDH

as an internal standard.

For immunoprecipitation analysis, lysates were premixed with the indicated antibodies and protein A/G beads (Santa Cruz Biotechnology, USA) overnight at 4 ℃. The immunoprecipitated protein complex was washed 5 times prior to western blotting analysis.

**Orthotopic transplantation tumor model**

For the orthotopic transplantation tumor model, CEMIP$^{OE}$-luc and Ctrl-luc MC38 were injected into the cecal wall after laparotomy in mice. The formation of orthotopic transplantation tumors was evaluated by small animal imaging technology (Caliper Life Sciences, USA).

**Immunohistochemistry**

Formalin-fixed paraffin-embedded (FFPE) tissue samples of 19 human primary colorectal cancer lesions were cut in serial sections (4 mm). FFPE sections were prepared for staining using standard protocols for xylene and alcohol gradient for deparaffination. Antigen retrieval was performed in the pressure cooker (95°C for 30 min) using Antigen Unmarking Solution to remove aldehyde links formed during the initial fixation of tissues. The slides were incubated with primary antibody (MHC-I, Proteintech, China, 1:1000; CEMIP, Proteintech, China, 1:200) overnight at 4C. After washing with PBS, the slides were incubated with peroxidase enzyme-conjugated secondary antibody for 30 minutes at 37℃. For quantitative assessment, Image J software was used to measure the positive staining area, and the average ratio of 5

microscopic fields (original magnification, ×200) was calculated.

**Supplementary Figure legends**

**Figure S1 The effect of CEMIP on tumor cell growth in vitro and in vivo (A)** Soft agar analysis of the colony-formation ability of vector control (Ctrl) or CEMIP-overexpressing ($CEMIP^{OE}$) MC38 cells. A quantitative representation of soft agar formation is shown. n = 3 independent experiments. **(B-C)** Vector control (Ctrl) or CEMIP-overexpressing ($CEMIP^{OE}$) MC38 or CT26 cells were injected subcutaneously into C57BL/6 mice or Balb/c mice, respectively. The tumor image (B) and tumor weight (C) were collected. Scale bars, 1 cm. n = 6/group. **(D)** Representative bioluminescent imaging (BLI) of the 20-day tumor growth assay after Ctrl and $CEMIP^{OE}$ MC38 tumor cells orthotopically transplanted into the subserosa of the cecum of C57BL/6 mice. All data are shown as the mean ± s.e.m. ns, not significant. **(E)** Gating strategies for flow cytometry analysis of tumors used in this study. **(F)** Immunofluorescence staining (left) and quantitative estimates (right) of $CD8^+$ T cells in vector control and $CEMIP^{OE}$ CT26 tumors. Scale bar 20 μm. n = 3 independent samples; four fluorescent fields of each sample were counted by ImageJ. $P<0.05$ represents statistically significant. **(G)** The percentages of $Ki67^+$ $CD8^+$ T cells in vector control and $CEMIP^{OE}$ MC38 and CT26 tumors were analyzed by flow cytometry.

**Figure S2 Additional data on the characterization of lymphocyte infiltration into murine tumors and the effect of CEMIP on CD8$^+$ T cell function (A)** Quantitative estimates of CD4$^+$, CD8$^+$T cells and NK cells in the spleens of mice bearing control and CEMIP$^{OE}$ MC38 tumors, as determined by flow cytometry. n = 6/group; Mean ± s.e.m. **(B)** The percentages of tumor-infiltrating CD3$^+$, CD4$^+$, Treg and NK cells were analyzed by flow cytometry. Mean ± s.e.m., n = 4-5/group. **(C)** Left, negative correlation of CEMIP mRNA levels with active-CD8$^+$ T (Act_CD8) cells in human CRC; Right, there is no significant correlation of CEMIP mRNA levels with central memory CD8$^+$ T cells (Tcm_CD8) in human CRC. Associations of the CEMIP expression level with lymphocytes in CRC derived from the Tumor and Immune System Interaction Database (TISIDB). **(D)** GSEA using the TCGA CRC database showed the correlation of CEMIP protein expression with the T cell activation signature. **(E-F)** MC38 cells with different CEMIP expression levels (Ctrl-sh or CEMIP$^{KD}$) were co-cultured with T cells, and cell apoptosis was determined by flow cytometry analysis. After 72 h, cell apoptosis was determined by 7-AAD$^+$ (E), and T cells proliferation was measured by CFSE dilution (F). n = 3 biological replicates. Mean ± s.e.m., $P$<0.05 represents statistically significant.

**Figure S3 CD8$^+$T cells depletion experiment. (A)** The efficiency of CD8+ T cells clearance was confirmed by flow cytometry. **(B-C)** Tumor images (B) and tumor weight (C) of Ctrl-sh and CEMIP$^{KD}$ MC38 after treatment with a neutralization antibody against CD8.

**Figure S4 The effect of CEMIP on promoting the degradation of MHC-I (A)** The expression of CEMIP and MHC-I (HLA-A, -B) in several human colon cancer cells was determined by western blotting. **(B)** Surface MHC-I (HLA-A/B/C) was measured by flow cytometry in several human colon cancer cell lines. **(C)** Quantitative reverse transcription PCR (qRT–PCR) analysis of MHC-I (HLA-A, HLA-B) in control and $CEMIP^{OE}$ SW480 cells. **(D)** Surface PD-L1 was measured by flow cytometry in Ctrl and $CEMIP^{OE}$ MC38 cells. **(E)** The expression of MHC-I (green) and CEMIP (red) in colon cancer patients was determined by Immunofluorescence. Representative images of 2 patients were shown. Scale bar, 500 μm. All data are shown as the mean ± s.e.m. ns, not significant.

**Figure S5 CEMIP restricted $CD8^+$ T cell cytotoxicity partially due to impaired MHC-I expression. (A-B)** CT26-OVA cells were co-cultured with $CD8^+$ T cells isolated from Balb/c mice with control isotype or MHC-I blocking antibody. $CD8^+$ T proliferation was measured by CFSE dilution (A), and the secretion of the cytokines granzyme $B^+$ and IFN-$\gamma^+$ was analyzed by flow cytometry (B). All data are shown as the mean ± s.e.m. n = 3 biological replicates.

**Figure S6 CEMIP promotes MHC-I internalization via clathrin-mediated endocytosis (A)** Immunofluorescence quantification of MHC-I in the cytosolic and plasma membrane fractions of $CEMIP^{OE}$ and Ctrl SW480 cells. n = 3 independent experiments; four fluorescent fields for each of the three samples were counted by ImageJ. Scale bars, 5 μm. **(B)** $CEMIP^{OE}$ MC38 cells were treated with different

endocytosis inhibitors at the indicated concentrations. Clathrin inhibitor (chlorpromazine, CPZ), caveolae inhibitor (MβCD), Arf6 inhibitor (NVA-2729) or cdc42 inhibitor (ZCL278). Then, the MHC-I levels in the intracellular versus plasma membrane (PM) were analyzed by flow cytometry. n = 3 independent experiments. **(C)** The expression of clathrin in MC38 or CT26 cells transfected with three different clathrin siRNAs or control siRNA. SC, cells treated with control scrambled siRNA. **(D)** Surface H-2K$^{b}$ was measured by flow cytometry in CEMIP-knockdown (CEMIP$^{KD}$) MC38 and CT26 cells transfected with siRNA clathrin or control siRNA. **(E-G)** Tumor growth was monitored in Balb/c mice bearing Ctrl and CEMIP$^{OE}$ CT26 cells treated with the clathrin inhibitor CPZ and the lysosome inhibitor CQ. Tumor image (E), volume (F), and weight (G) are shown. n = 5/group. **(H)** Schematic diagram of CEMIP protein deletion mutants (A:1−303aa, B: 295−591aa, C: 572−819aa, D: 820-1204 aa, E:1205-1361 aa) with a C-terminal MYC tag. Data are shown as the mean ± s.e.m. $P<0.05$ represents statistically significant. ns, not significant.

**Figure S7 The effect of CEMIP on anchoring MHC-I to lysosomes for degradation**

**(A)** Confocal micrographs of Ctrl and CEMIP$^{OE}$ SW480 cells stained for H-2K$^{b}$ and LAMP1 markers. Scale bar, 20 μm. Bar graphs depict % colocalization shown for the respective markers in boxed insets (Manders'coefficient). **(B)** Representative flow cytometry images of surface MHC-I (H-2K$^{b}$) levels in CEMIP-overexpressing and CEMIP-knockdown MC38 cells treated with 150 nM bafilomycin A1 (BafA1) for the

indicated time. **(C)** CEMIP knockdown attenuates the ubiquitination of MHC-I. Ctrl and $CEMIP^{KD}$ SW480 cells were transduced with HA-UB plasmids. MHC-I molecules were immunoprecipitated, and their ubiquitination status was determined by western blotting analysis using an anti-HA antibody.

**Figure S8 CEMIP inhibition increases the sensitivity of colon cancer cells to immune checkpoint blockade (A-D)** C57BL/6 mice were implanted with $3\times10^5$ Ctrl or $CEMIP^{KD}$ cells and received PD-1 mAb treatment plus CTLA-4 mAb or IgG isotype control (IgG). A schematic view of the treatment plan (A), tumor image (B), tumor volume (C), and tumor weight (D) were measured every 2 days. n=5 mice per group. **(E)** Tumors from the above mice were collected. The Abundance of tumor-infiltrating $CD8^+$ T cells normalized by MC38 tumor weight per gram (left). The percentages of IFN-$\gamma^+$ (middle) and $GZMB^+$ $CD8^+$ (right) T cells were analyzed by flow cytometry. **(F)** The expression of CTLA-4 and PD-1 by the intratumoral $CD8^+$ T cells was analyzed by flow cytometry. **(G)** CEMIP gene expression levels in TCGA colorectal adenocarcinoma tumors, according to MSI status. MSI, microsatellite instability; MSI-H, MSI-high; MSI-L, MSI-low; MSS, microsatellite stable. $P<0.05$ represents statistically significant.

| Gene | Directions | Sequences |
|---|---|---|
| siRNA Control | sense | UUCUCCGAACGUGUCACGUTT |
| | antisense | ACGUGACACGUUCGGAGAATT |
| siRNA *clathrin*#1 | sense | GCAUCUACAUGAACAGAAUTT |
| | antisense | AUUCUGUUCAUGUAGAUGCTT |
| siRNA *clathrin*#2 | sense | CCUUCUUACUUGAUGCUUUTT |
| | antisense | AAAGCAUCAAGUAAGAAGGTT |
| siRNA *clathrin*#3 | sense | GCUCAUCAAUGUUUGCAAUTT |
| | antisense | AUUGCAAACAUUGAUGAGCTT |
| HLA-A | forward | GACGCCGCGAGCCAG |
| | reverse | GCGATGTAATCCTTGCCGTCG |
| HLA-B | forward | TCTCCTCAGACGCCGAGATGC |
| | reverse | CTGTCTCAGGCTTTTCAAGCTG |
| GAPDH | forward | GCUCUUUGAGGACAACUAUTT |
| | reverse | AUAGUUGUCCUCAAAGAGCTT |

**Table S1. SiRNA sequences or primers used in this study**

| **Antibodies** | **Supplier** | **Reference** |
|---|---|---|
| HLA-A, B, C | Santa Cruz | sc-271388 |
| HLA-A | Abacm | ab52922 |
| HLA-B | Abacm | ab193415 |
| Purified anti-mouse H-2K$^{b}$ | Biolegend | 116501 |
| Purified anti-mouse H-2K$^{d}$ | Biolegend | 116601 |
| CEMIP | Proteintech | 21129-1-AP |
| GAPDH | Proteintech | 60004-1-Ig |
| Clathrin | Proteintech | 26523-1-AP |
| $Na^{+}K^{+}$/ATPase | Proteintech | 14418-1-AP |
| LAMP1 | Abcam | Ab108597 |
| EEA1 | Abcam | Ab109110 |
| Rab7 | Abacm | Ab126712 |
| PerCP anti-mouse CD45 | Biolegend | 103129 |
| FITC anti-mouse CD3 | Biolegend | 317306 |
| PE anti-mouse CD4 | Biolegend | 980804 |
| PE anti-mouse NK | Biolegend | 108907 |
| BV510 anti-mouse CD8 | Biolegend | 344732 |
| APC anti-mouse FOXP3 | Invitrogen | 77-5775-40 |
| BV421 anti-mouse IFN-γ | Biolegend | 505829 |

| | | |
|---|---|---|
| PE/Dazzle™ 594 anti-mouse/human Granzyme | Biolegend | 372215 |
| Alexa Fluor® 647 anti-mouse H-2K$^{b}$ | Biolegend | 116512 |
| APC anti-mouse H-2K$^{d}$ | Biolegend | 116619 |
| BV605 anti-mouse PD-1 | Biolegend | 367425 |
| APC anti-mouse CTLA-4 | Biolegend | 106309 |
| PE anti-mouse Ki67 | Biolegend | 652403 |
| InvivoMAb anti-mouse PD-1 | BioXcell | BE0146 |
| InvivoMAb anti-mouse CTLA-4 | BioXcell | BP0032 |
| InvivoMAb anti-mouse H-2K$^{b}$ | BioXcell | BE0121 |
| InVivoMAb mouse IgG1 isotype | BioXcell | BE0083 |

**Table S2. All antibodies used in this study**

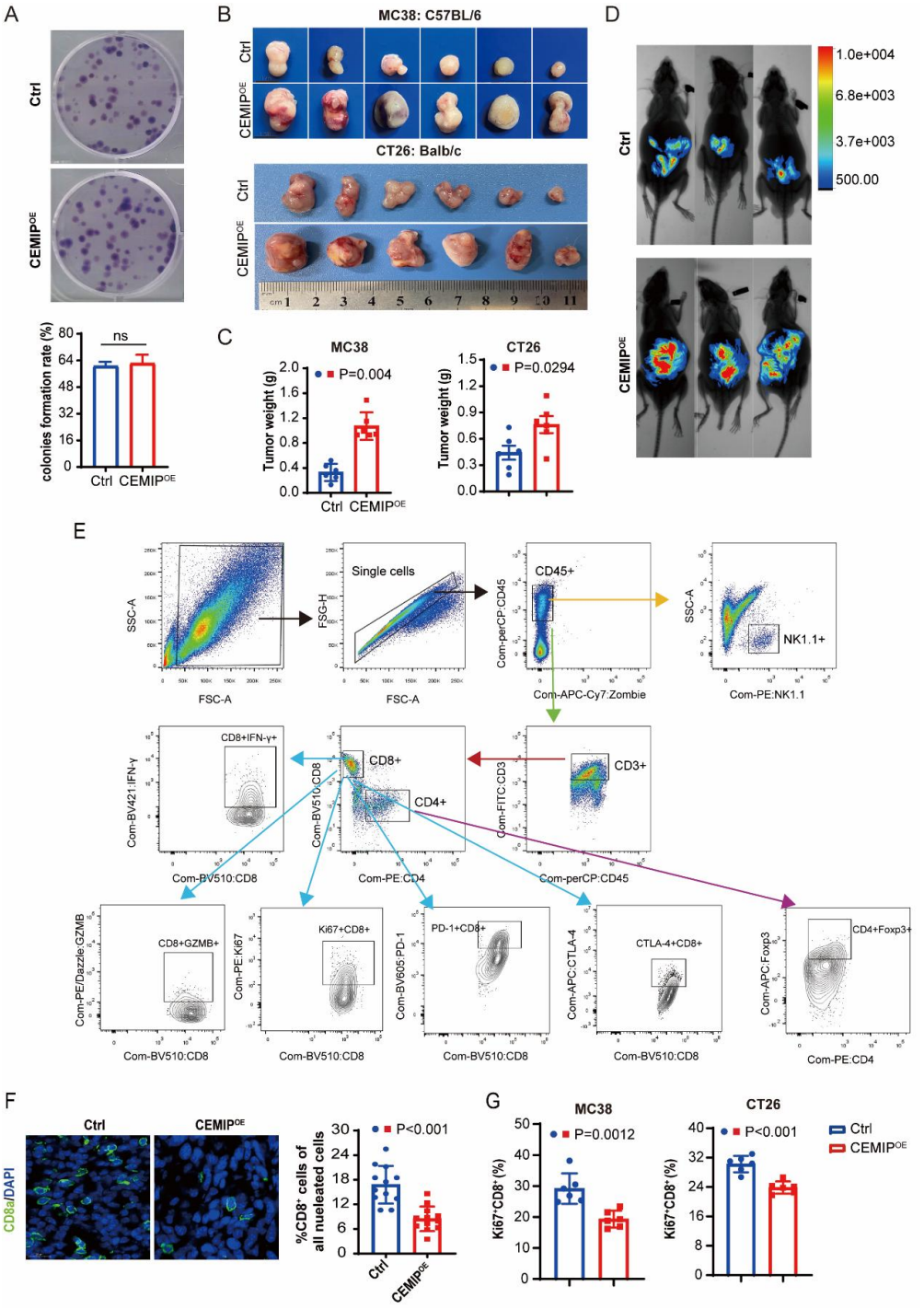
A
Ctrl
CEMIP^OE
colonies formation rate (%)
ns
Ctrl CEMIP^OE
B
MC38: C57BL/6
CT26: Balb/c
C
MC38
P=0.004
CT26
P=0.0294
Tumor weight (g)
D
1.0e+004
6.8e+003
3.7e+003
500.00
E
Single cells
CD45+
NK1.1+
CD8+IFN-γ+
CD8+
CD4+
CD3+
CD8+GZMB+
Ki67+CD8+
PD-1+CD8+
CTLA-4+CD8+
CD4+Foxp3+
F
CD8a/DAPI
%CD8+ cells of all nucleated cells
P<0.001
G
MC38
P=0.0012
CT26
P<0.001
Ki67+CD8+ (%)

**Figure S1**

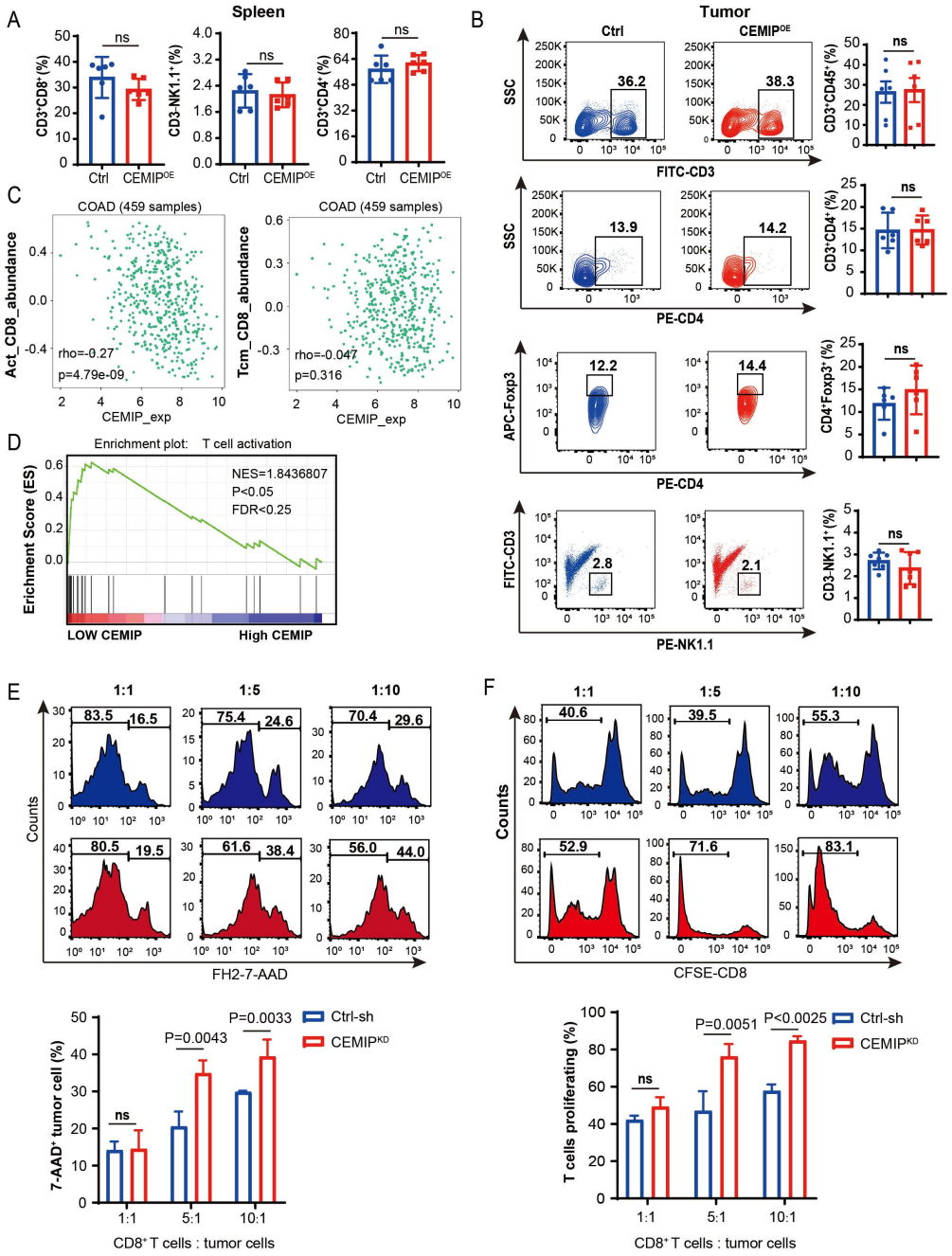
A
Spleen
CD3+CD8+ (%)
CD3-NK1.1+ (%)
CD3+CD4+ (%)
ns
Ctrl
CEMIPOE
B
Tumor
Ctrl
CEMIPOE
SSC
36.2
38.3
FITC-CD3
CD3+CD45+ (%)
13.9
14.2
PE-CD4
CD3+CD4+ (%)
12.2
14.4
APC-Foxp3
CD4+Foxp3+ (%)
2.8
2.1
PE-NK1.1
CD3-NK1.1+ (%)
C
COAD (459 samples)
Act_CD8_abundance
rho=-0.27
p=4.79e-09
CEMIP_exp
Tcm_CD8_abundance
rho=-0.047
p=0.316
D
Enrichment plot: T cell activation
Erichment Score (ES)
NES=1.8436807
P<0.05
FDR<0.25
LOW CEMIP
High CEMIP
E
1:1
1:5
1:10
Counts
83.5
16.5
75.4
24.6
70.4
29.6
80.5
19.5
61.6
38.4
56.0
44.0
FH2-7-AAD
7-AAD+ tumor cell (%)
P=0.0033
P=0.0043
Ctrl-sh
CEMIPKD
CD8+ T cells : tumor cells
F
40.6
39.5
55.3
52.9
71.6
83.1
CFSE-CD8
T cells proliferating (%)
P=0.0051
P<0.0025

**Figure S2**

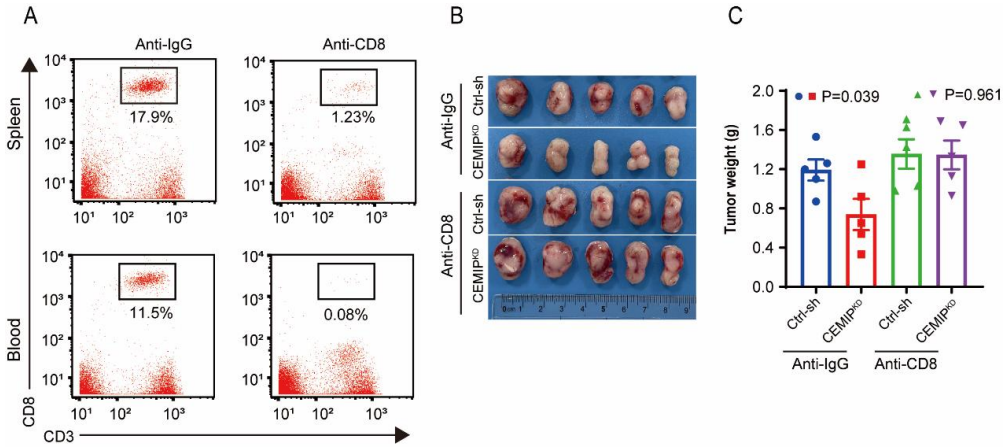
A
Anti-IgG
Anti-CD8
Spleen
Blood
17.9%
1.23%
11.5%
0.08%
CD8
CD3
B
Anti-IgG
Anti-CD8
Ctrl-sh
CEMIP^KD
C
P=0.039
P=0.961
Tumor weight (g)
2.0
1.6
1.2
0.8
0.4
0.0
Ctrl-sh
CEMIP^KD
Anti-IgG
Anti-CD8

**Figure S3**

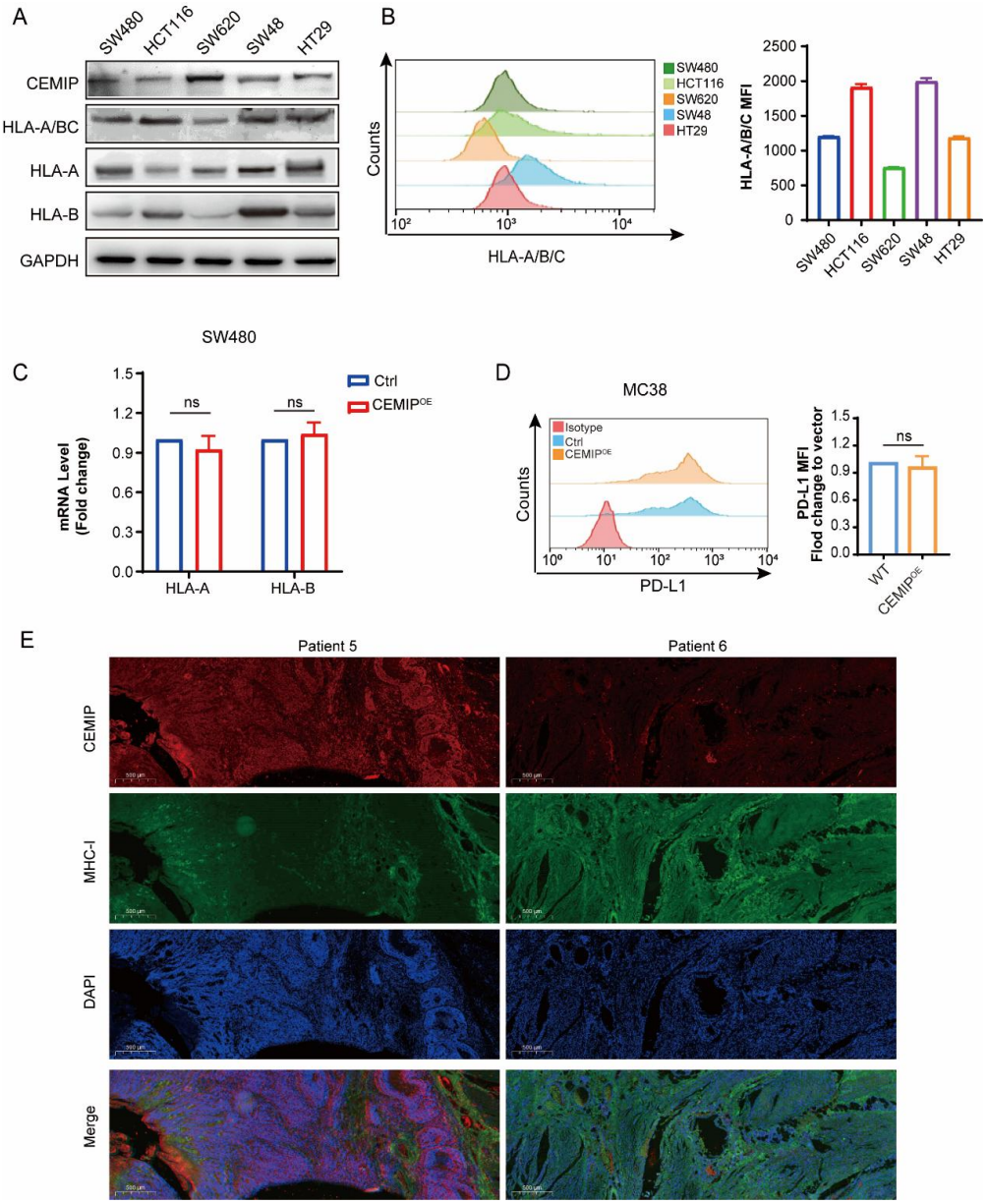
A
SW480
HCT116
SW620
SW48
HT29
CEMIP
HLA-A/BC
HLA-A
HLA-B
GAPDH
B
Counts
HLA-A/B/C
SW480
HCT116
SW620
SW48
HT29
HLA-A/B/C MFI
C
SW480
mRNA Level (Fold change)
ns
Ctrl
CEMIP^OE
HLA-A
HLA-B
D
MC38
Isotype
Ctrl
CEMIP^OE
Counts
PD-L1
PD-L1 MFI Flod change to vector
WT
CEMIP^OE
E
Patient 5
Patient 6
CEMIP
MHC-I
DAPI
Merge

**Figure S4**

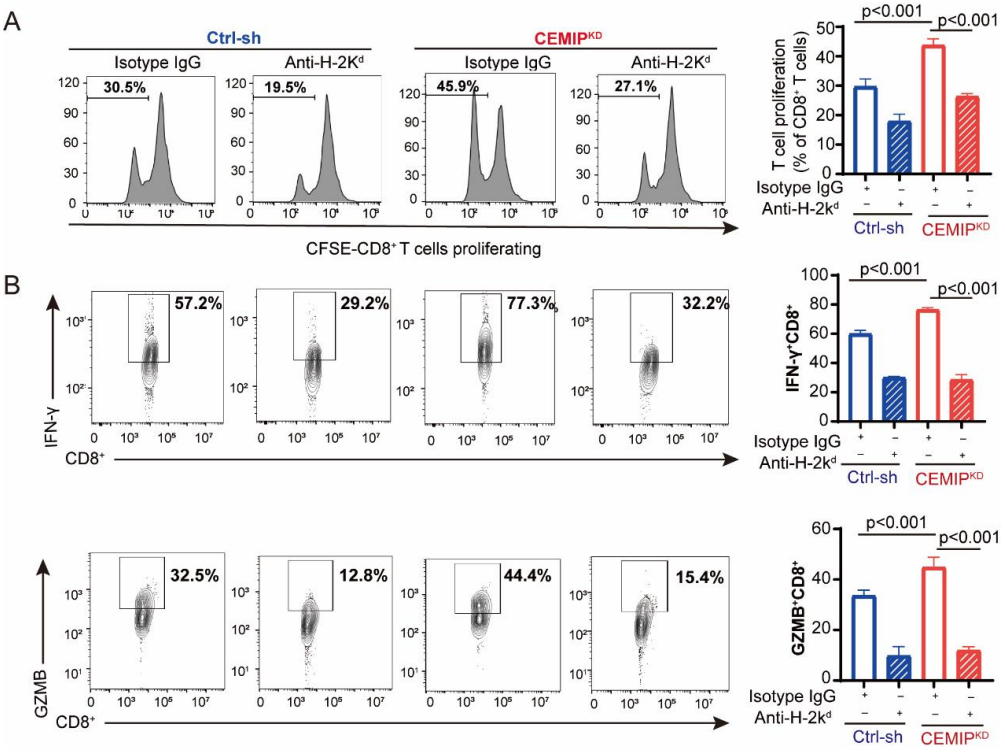
A
Ctrl-sh
CEMIP^KD
Isotype IgG
Anti-H-2K^d
30.5%
19.5%
45.9%
27.1%
CFSE-CD8+ T cells proliferating
T cell proliferation (% of CD8+ T cells)
p<0.001
p<0.001
Isotype IgG
Anti-H-2k^d
Ctrl-sh
CEMIP^KD
B
IFN-γ
CD8+
57.2%
29.2%
77.3%
32.2%
IFN-γ+CD8+
GZMB
32.5%
12.8%
44.4%
15.4%
GZMB+CD8+

**Figure S5**

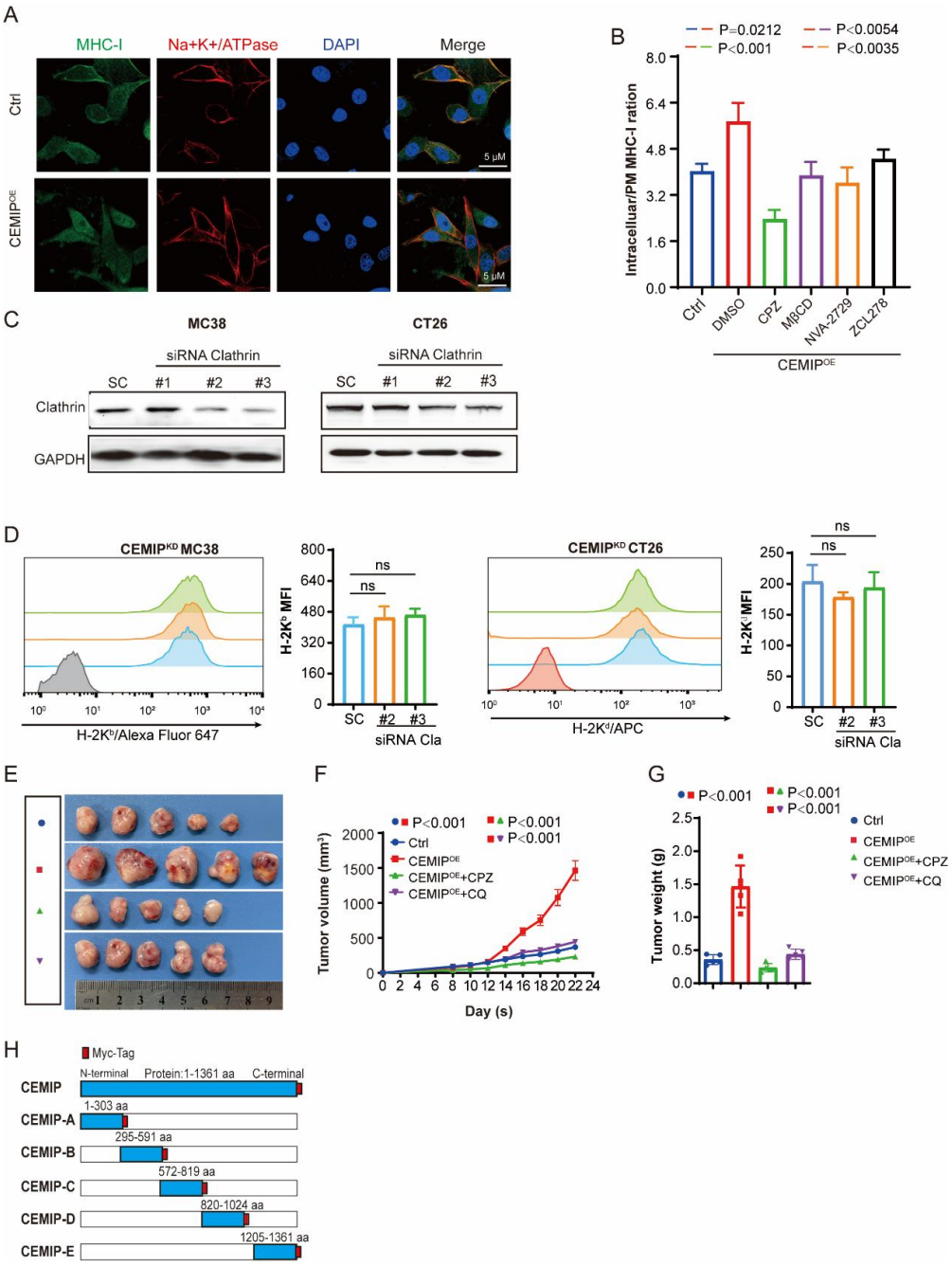
A
MHC-I
Na+K+/ATPase
DAPI
Merge
Ctrl
CEMIP^OE
5 μM
B
P=0.0212
P<0.0054
P<0.001
P<0.0035
Intracelluar/PM MHC-I ration
Ctrl
DMSO
CPZ
MβCD
NVA-2729
ZCL278
CEMIP^OE
C
MC38
CT26
siRNA Clathrin
SC
#1
#2
#3
Clathrin
GAPDH
D
CEMIP^KD MC38
CEMIP^KD CT26
H-2K^b MFI
H-2K^d MFI
ns
H-2K^b/Alexa Fluor 647
H-2K^d/APC
siRNA Cla
E
F
P<0.001
Ctrl
CEMIP^OE
CEMIP^OE+CPZ
CEMIP^OE+CQ
Tumor volume (mm³)
Day (s)
G
Tumor weight (g)
H
Myc-Tag
N-terminal
Protein:1-1361 aa
C-terminal
CEMIP
CEMIP-A
1-303 aa
CEMIP-B
295-591 aa
CEMIP-C
572-819 aa
CEMIP-D
820-1024 aa
CEMIP-E
1205-1361 aa

**Figure S6**

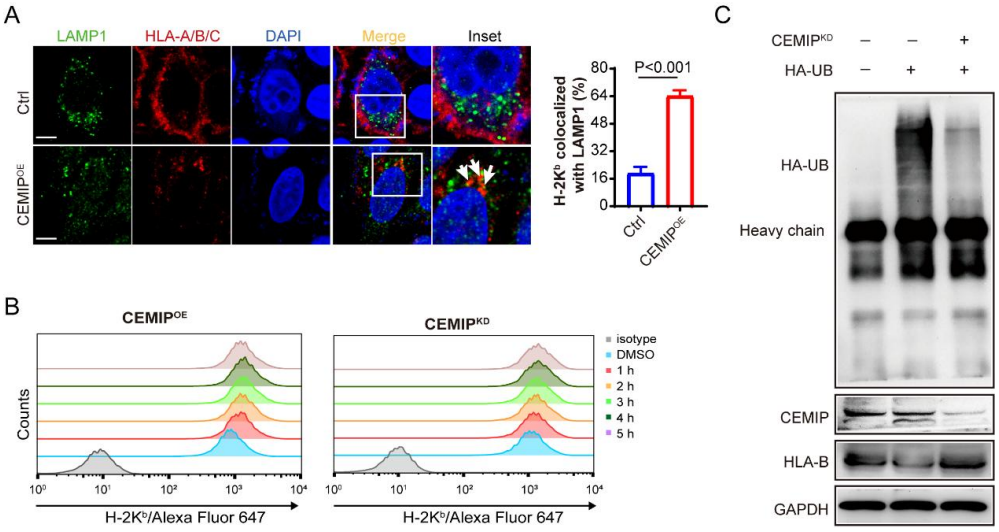
A
LAMP1
HLA-A/B/C
DAPI
Merge
Inset
Ctrl
CEMIPOE
P<0.001
H-2Kb colocalized with LAMP1 (%)
80
64
48
32
16
0
Ctrl
CEMIPOE
B
CEMIPOE
CEMIPKD
isotype
DMSO
1 h
2 h
3 h
4 h
5 h
Counts
H-2Kb/Alexa Fluor 647
H-2Kb/Alexa Fluor 647
C
CEMIPKD – – +
HA-UB – + +
HA-UB
Heavy chain
CEMIP
HLA-B
GAPDH

**Figure S7**

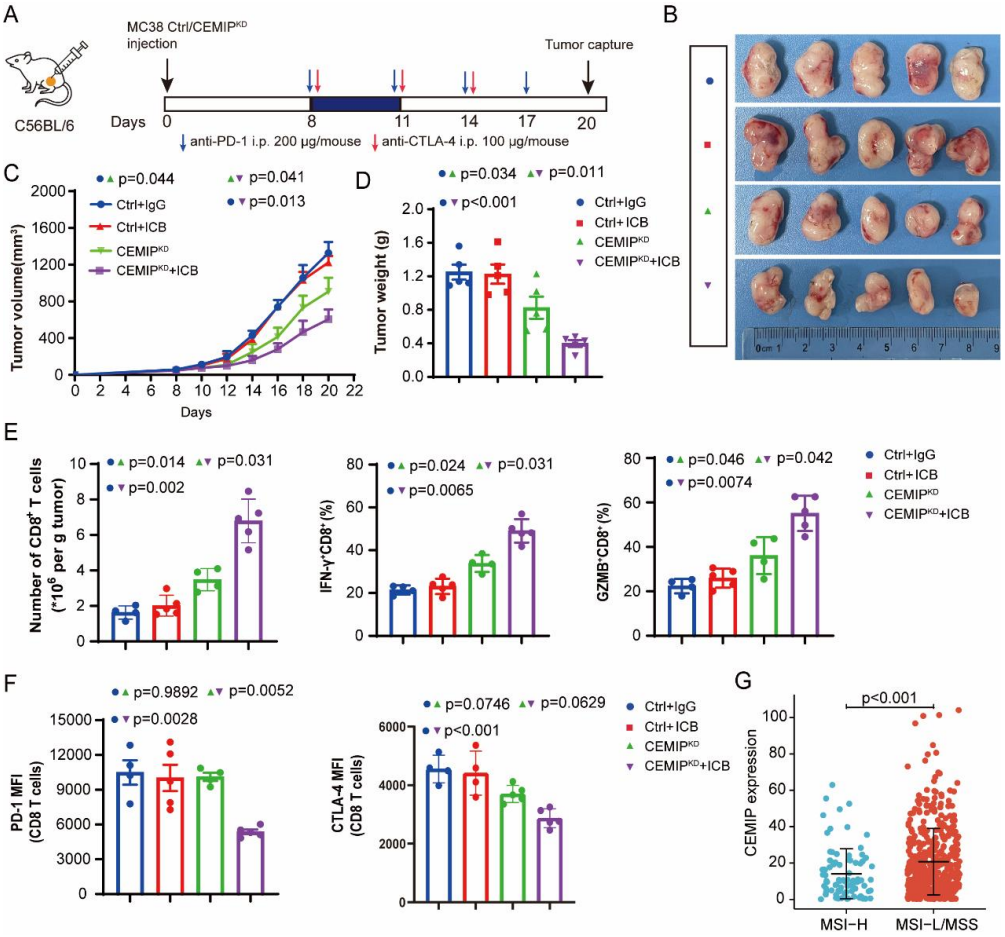
A
MC38 Ctrl/CEMIP^KD injection
Tumor capture
C56BL/6
Days 0 8 11 14 17 20
anti-PD-1 i.p. 200 μg/mouse
anti-CTLA-4 i.p. 100 μg/mouse
B
C
p=0.044
p=0.041
p=0.013
Ctrl+IgG
Ctrl+ICB
CEMIP^KD
CEMIP^KD+ICB
Tumor volume(mm³)
Days
D
p=0.034
p=0.011
p<0.001
Tumor weight (g)
E
p=0.014
p=0.031
p=0.002
Number of CD8⁺ T cells (*10⁶ per g tumor)
p=0.024
p=0.031
p=0.0065
IFN-γ⁺CD8⁺ (%)
p=0.046
p=0.042
p=0.0074
GZMB⁺CD8⁺ (%)
F
p=0.9892
p=0.0052
p=0.0028
PD-1 MFI (CD8 T cells)
p=0.0746
p=0.0629
p<0.001
CTLA-4 MFI (CD8 T cells)
G
p<0.001
CEMIP expression
MSI-H
MSI-L/MSS

**Figure S8**